Chemical and Process Engineering 2013, 34 (2), 269-282
DOI: 10.2478/cpe-2013-0022

CFD MODELLING OF CO_2 CAPTURE IN A PACKED BED BY CHEMICAL ABSORPTION

Dariusz Asendrych*, Paweł Niegodajew, Stanisław Drobniak

Czestochowa University of Technology, Institute of Thermal Machinery, al. Armii Krajowej 21, 42-200 Czestochowa, Poland

The paper deals with numerical modelling of carbon dioxide capture by amine solvent from flue gases in post-combustion technology. A complex flow system including a countercurrent two-phase flow in a porous region, chemical reaction and heat transfer is considered to resolve CO_2 absorption. In order to approach the hydrodynamics of the process a two-fluid Eulerian model was applied. At the present stage of model development only the first part of the cycle, i.e. CO_2 absorption was included. A series of parametric simulations has shown that carbon dioxide capture efficiency is mostly influenced by the ratio of liquid (aqueous amine solution) to gas (flue gases) mass fluxes. Good consistency of numerical results with experimental data acquired at a small-scale laboratory CO_2 capture installation (at the Institute for Chemical Processing of Coal, Zabrze, Poland) has proved the reliability of the model.

Keywords: carbon dioxide, carbon capture and storage (CCS), 2-phase flow, chemical absorption, computational fluid dynamics (CFD)

1. INTRODUCTION

Continuously growing CO_2 emission is one of the most important threats of today's power industry. Three technologies are currently available for carbon capture and storage (CCS), namely:

- pre-combustion capture - removal of CO_2 from decarbonised and gasified fuel (heating value transferred to hydrogen),
- oxy-fuel combustion - burning of fuel in oxygen atmosphere with CO_2 and water vapour as easily separable combustion products (Zhao et al., 2010),
- post-combustion - removal of CO_2 from flue gases (Lawal et al., 2010).

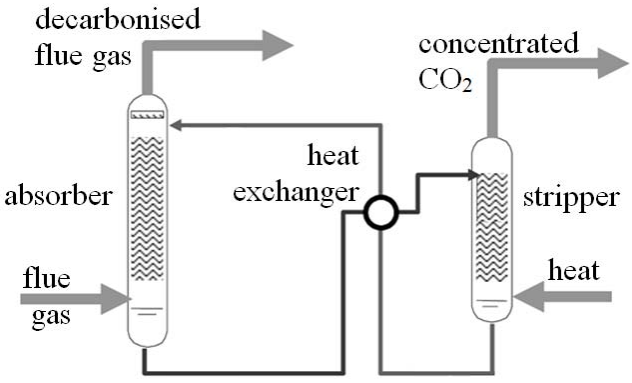

Fig. 1. The process flow diagram for CO_2 amine absorption

*Corresponding author, e-mail: darek@imc.pcz.czest.pl

In the post-combustion approach, being at present the preferred option of CO_2 capture (Lawal et al., 2010), flue gases are sent through an absorber where carbon dioxide is separated by chemical absorption using an aqueous amine solution flowing countercurrently. A process flow diagram for amine absorption is presented in Fig. 1. The flue gas enters the absorber at the bottom, whereas the solvent is released at the top of the column. Both phases pass through the packed bed, where most of the chemical reaction occurs due to an enlarged contact area between phases. A solution with CO_2 is pre-heated before entering the stripper where, through the addition of heat, the reaction is reversed. Desorbed CO_2 is then compressed and transported to a storage location. The recycled solvent is then pumped back to the absorber completing the process cycle. Monoethanolamine (MEA) is the most common choice of a chemical solvent used for these purposes, mainly due to its high reactivity (Alie, 2004) and the existing comprehensive data base of its physical and chemical properties (Kothandaraaman et at., 2009; Moser et al., 2011). Most of the present research of CCS technology is performed in two ways:

- experimentally using laboratory or pilot small-scale CC installations,
- simulating the process by means of 0D commercial codes, mainly ASPEN (Alie, 2004; Kothandaraaman et at., 2009) and gPROMS (Harun et al., 2011; Lawal et al., 2010) or 1D rate based models (e.g. Simon et al., 2011).

Although continuous progress in CCS technology has been observed in recent decade, it is still extremely expensive, as it decreases overall efficiency of the power cycle by approximately 30%. In order to make carbon capture commercially attractive, further significant progress should be made. It is believed that CFD modelling will provide a sufficient insight into absorption processes allowing for their further optimisation and noticeable reduction of costs. With the 2D axisymmetric CFD model it will be possible to capture the effects related to transverse mass, momentum and energy transfer processes, the inhomogeneity of the packed bed and the accumulation of liquid phase in the near-wall regions (see e.g. Basu, 2001). The model will also make it possible to test different designs of absorber column elements, e.g. liquid distributor, and their influence on the process performance. All these features cannot be included when simplified approaches (0D or 1D models) are employed to model the process.

The present paper deals with numerical modelling of CO_2 capture process, treated as a complex phenomenon including hydrodynamics of a coutercurrent gas-liquid two-phase flow in a porous region, chemical reaction and thermal effects due to its exothermic character (Asendrych et al., 2012). The simulation is a part of a larger project, including also the experimental investigations. For that purpose a small-scale laboratory installation has been designed and made operational at the Institute for Chemical Processing of Coal (IChPW) in Zabrze. The results of experimental trials (Krótki et al., 2012) are used for testing and validating the carbon dioxide capture numerical model being developed.

The paper is organised as follows: Section 2 includes a description of the numerical model, including geometry and boundary conditions, governing equations, absorption chemistry and the numerical tools used for the simulations. In Section 3 the detailed results of the process simulations are presented: flow hydrodynamics (subsection 3.1) and absorption process (subsection 3.2) for the nominal process conditions, analysis of varying amine solution composition on absorber performance (subsection 3.3), and finally a comparison of numerical results with experimental data from the laboratory CCS installation (subsection 3.4). The paper is summarised in Section 4.

2. MODEL DESCRIPTION

2.1. Problem Formulation

The present numerical study is focused on the simulation of CO_2 absorption process, i.e. the first stage

of CCS technology, which takes place in the absorber column (see Fig. 2a). Its model (see Fig. 2b) follows the geometry and dimensions of a laboratory CCS installation at IChPW. The column is of a cylindrical shape with a diameter of 0.1m and height of 1.5m (Krótki et al., 2012). A working absorber section filled with packing elements, 1.2m high, is placed in the centre of the column. Standard Raschig rings 6mm were used as a packing material with a porosity (called also void fraction) $\varepsilon = 0.8$ and surface area 789m^2/m^3. The only detail differing the real column and the model geometry is the liquid distributor. In the simulation liquid is supplied to the packed bed uniformly at the cross section (see Fig. 2b), while in the laboratory installation it is supplied as a liquid screen of a width of 2mm at the radial coordinate equal to the half of the column radius. It is believed, however, that the way of amine solution supply may only insignificantly influence the process. The nominal fluxes of media in the column are: 5m^3/h and 0.05m^3/h of flue gas and MEA solution, respectively. The flow intensity of the gaseous phase (dominating one) results in the Reynolds number of about $Re = 1400$ and $Re = 50$ outside and inside the porous region, respectively. Such a flow corresponds to the inertial-laminar flow regime (see Crespy et al., 2007). The composition of both media used in the simulations corresponded to the experimental trials conducted with the laboratory installation at IChPW. It should be noted that the carbonised gases used at the present stage of the project were produced in an artificial way instead of using flue gases from combustion chambers. For CO_2 absorption an aqueous solution of primary amine was used with 20% mass content and some chemical additives prohibiting the solution from corrosion and foaming. The operational parameters of the column including media composition are collected in Tab. 1.

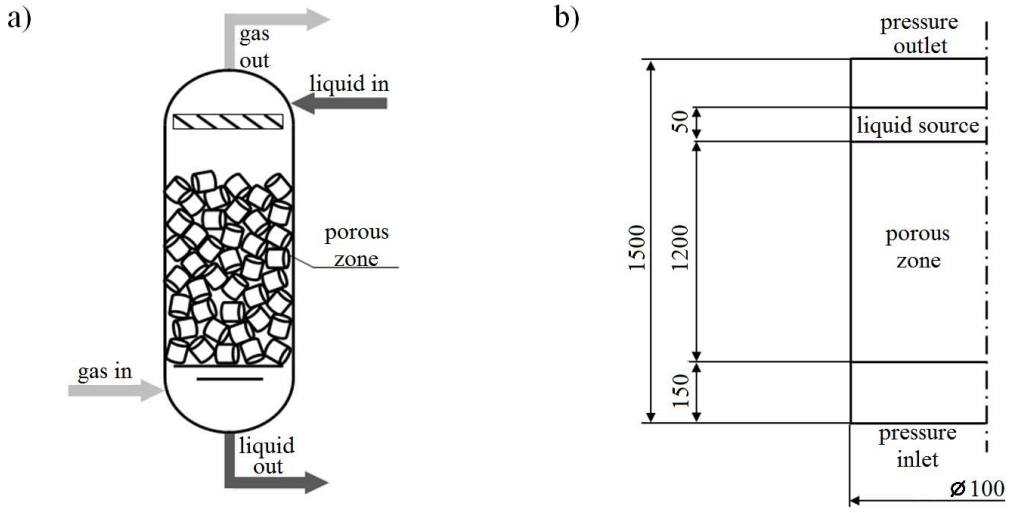

Fig. 2. Sketch of the absorber column (a), geometry and boundary conditions applied in the model (b)

Table 1. Operating parameters of media

		flue gas		liquid solvent	
flux	m^3/h	5		0.05	
mass content	%	air	87.1	H_2O	78.85
		CO_2	11.4	MEA	20
		H_2O vapour	1.5	additives	1.15

The actual material properties of media were implemented, in particular dynamic viscosity and density of monoethanolamine were taken from Weiland et al. (1998), as these properties vary significantly with temperature, CO_2 loading (number of moles of CO_2 per mole of amine) and mass MEA content in a liquid mixture.

The model of the absorber column was developed as a 2-dimensional axi-symmetric, laminar and unsteady multiphase gas-liquid flow. The 2-fluid Euler-Euler approach was implemented to describe the two-phase countercurrent flow. The boundary conditions of the model are presented in Fig. 2. The pressure inlet and pressure outlet boundaries were assigned suitably to the bottom and the top of the column. Such a setup allows the phases to leave freely the domain. The flue gas enters the column at its bottom and an aqueous solution of MEA is released from the source located at the top of the porous region. These types of boundary conditions have been found to ensure the convergence of the solution (Xu et al., 2008).

2.2. Governing equations

In the Euler-Euler multiphase approach fluid phases are treated as interpenetrating continua. In order to describe the coexistence of different phases in the flow the concept of volumetric fraction is introduced. The volume fractions for all the phases have to sum up to unity

$$\sum \alpha_k = 1 \tag{1}$$

Conservation equations are formed for each phase separately. The equation of mass conservation for k^{th} phase takes the form

$$\frac{\partial}{\partial t}(\alpha_k \rho_k) + \nabla \cdot (\alpha_k \rho_k \boldsymbol{u}_k) = S_k \tag{2}$$

where $\boldsymbol{u}_k$ is the velocity vector, ρ_k phase density and S_k is a mass source term corresponding to species production/destruction due to chemical reaction. The momentum equation for k^{th} phase with respect to the Eulerian multiphase model (assuming flow incompressibility) has the following form:

$$\frac{\partial}{\partial t}(\alpha_k \rho_k \boldsymbol{u}_k) + \nabla(\alpha_k \rho_k \boldsymbol{u}_k \boldsymbol{u}_k) = -\alpha_k \nabla p + \nabla^2(\alpha_k \mu_k \boldsymbol{u}_k) + \alpha_k \rho_k \boldsymbol{g}_k + \boldsymbol{F}_k + \boldsymbol{S}_{pz,k} \tag{3}$$

where p is the static pressure shared by all phases, μ_k stands for dynamic viscosity, $\boldsymbol{g}_k$ is the gravity vector and $\boldsymbol{F}_k$ describes an interaction force between phases. In the porous region, being the most important absorber column section, the additional flow resistance $\boldsymbol{S}_{pz,k}$ occurs

$$\boldsymbol{S}_{pz,k} = \frac{\mu_k}{\varsigma_k}\boldsymbol{u}_k + C_k \frac{1}{2}\rho_k |\boldsymbol{u}_k| \boldsymbol{u}_k \tag{4}$$

where the first term on the right hand side is the viscous loss term, while the second one corresponds to the inertial momentum loss. The values of these coefficients were determined in an experimental way for the air flow in a dry column and were believed to be nearly constant for the low volume fraction levels.

The phase interaction force $\boldsymbol{F}_k$ appearing in Eq. (3) has been defined with a formula proposed in Schiller and Naumann (1935), which adequately describes the interactions of dispersed phases (i.e. droplets or bubbly flows). By adjusting the length scale of the liquid phase it was possible to obtain realistic flow behaviour of countercurrent streams, i.e. a typical level of liquid volume fraction for this kind and size of packing elements (Billet, 1995). However, it is planned to adopt a more relevant mechanism, specific for gas-liquid film systems, which has been reported in the literature (e.g. Billet, 1995).

For the reacting system, additional governing equations have to be included in the model. General transport equation of i^{th} species in multiphase flow can be given as

$$\frac{\partial}{\partial t}(\alpha_k \rho_k Y_{i,k}) + \nabla \cdot (\alpha_k \rho_k \boldsymbol{u}_k Y_{i,k}) = -\nabla \cdot (\alpha_k \boldsymbol{J}_{i,k}) + R_i \tag{5}$$

where $Y_{i,k}$ is the mass fraction, R_i stands for the heterogeneous reaction rate and $\boldsymbol{J}_{i,k}$ is a stream of the i^{th} species due to diffusion. In laminar flow the diffused flux can be described by the Fick's law

$$\boldsymbol{J}_{i,k} = \alpha_k \rho_k D_{i,M} \nabla Y_{i,k} - D_{i,T} \frac{\nabla T}{T} \tag{6}$$

with $D_{i,m}$ and $D_{i,T}$ denoting the mass and thermal diffusion coefficients of the i^{th} species in the mixture, respectively. To describe the energy transfer in Eulerian model, a separate enthalpy equation is solved for k^{th} phase

$$\frac{\partial}{\partial t}(\alpha_k \rho_k h_k) + \nabla \cdot (\alpha_k \rho_k \boldsymbol{u}_k h_k) = \alpha_k \frac{\partial p}{\partial t} + \nabla \cdot (\lambda_k \nabla T_k) + Q_k + S_{e,k} \tag{7}$$

where h_k is the specific enthalpy of the k^{th} species, λ_k stands for thermal conductivity, Q_k is the intensity of heat exchange between phases and $S_{e,k}$ is the enthalpy source term due to chemical reaction.

2.3. Absorption chemistry

The chemistry of CO_2 absorption by aqueous monoethanolamine solution is usually described by a system of several equilibrium reversible reactions. However, for typical operating conditions of absorber columns the process may be regarded as a non-reversible one and approximated with sufficient accuracy by the 2-step reaction mechanism (Astarita et al., 1983; Vaidya and Kenig, 2007). At first, the so-called zwitterion is formed by absorption CO_2 by amine molecule

$$CO_2 + RNH_2 \rightarrow RNH_2^+ COO^- \tag{8a}$$

and then it undergoes deprotonation by the second amine molecule

$$RNH_2^+ COO^- + RNH_2 \rightarrow RNHCOO^- + RNH_3^+ \tag{8b}$$

resulting in carbamate formation. In the above reactions R represents an alcanol group $(CH_2)_2OH^-$. Expressions (8) neglect the presence of ions (such as H_30^+, OH^-, CO_3^{2-}) as their content for CCS installations working on fossil fuels with MEA as a solvent is very low. The mass rate of i^{th} chemical species produced due to the heterogeneous second-order reaction is given by:

$$R_i = M_i \cdot k_f \cdot C_{MEA} \cdot C_{CO2} \tag{9}$$

where M_i is the molecular weight, k_f is a forward reaction rate constant and C_{MEA} and C_{CO2} stand for molar concentrations of reacting media, i.e. MEA and carbon dioxide, respectively. The reaction constant may be approximated by the following expression:

$$log(k_f) = 10.99 - 2152 / T \tag{10}$$

which was obtained experimentally by Barth et al. (1986).

2.4. Numerical tools and procedures

The model of the absorber column was developed in ANSYS FLUENT 13, a commercial CFD code. The Eulerian/Eulerian approach was implemented to describe the two-phase counter-current flow. In order to ensure high accuracy of computations 2nd order discretisation schemes were applied. For the pressure correction SIMPLE scheme was used. The convergence of the solution for each time step was controlled with residua, for energy equation it had to fall below the level of 10^{-6} while for the remaining equations the value of 10^{-3} was accepted. The calculation procedure was split into 2 stages, i.e. at first the simulation was being conducted with velocity inlet boundary condition for gas phase and no liquid present in the domain. After achieving the convergent quasi-steady gas flow, the gas inlet boundary

condition was replaced by pressure inlet and the liquid phase started to be released from the liquid source, making finally the 2-phase flow. The details of the calculation procedure of the gas-liquid mixture in countercurrent flow system were described in Niegodajew and Asendrych, 2012.

The geometry and numerical grid was created in ANSYS GAMBIT - FLUENT's pre-processor. Numerous variants of meshing strategies as well as several grid sizes were investigated in order to determine the most optimal mesh allowing minimised numerical diffusion. In order to satisfy different requirements of particular column sections the 2-step procedure was applied. First, a structured mesh was created for the entire geometry with adequate cell density in the near-wall regions. Then, the mesh was conditionally refined in the sections outside the porous zone in the flow regions of high velocity gradients. A series of test calculations has shown that the mesh size of approximately 13,000 cells provided the best compromise between accuracy and computational speed.

3. SIMULATION RESULTS

The numerical model described in detail in Chapter 2 was employed to simulate CO_2 absorption for the nominal conditions, presented in Tab. 1. The results of simulations showed a physically justified behaviour of the absorber column and typical distributions of process key parameters, described in the following sections.

3.1. Flow Hydrodynamics

At first, the results of flow hydrodynamics are presented and discussed. In Fig. 3 the axial distributions of static pressure p, gas u_g and liquid u_l velocities as well as volume fraction of liquid phase α_l are shown. One can easily note that the static pressure drops practically in the porous region only (see Fig. 3a), and beyond that zone pressure changes are negligible. It shows the importance of the flow resistance term appearing in this region (see Eq. 4).

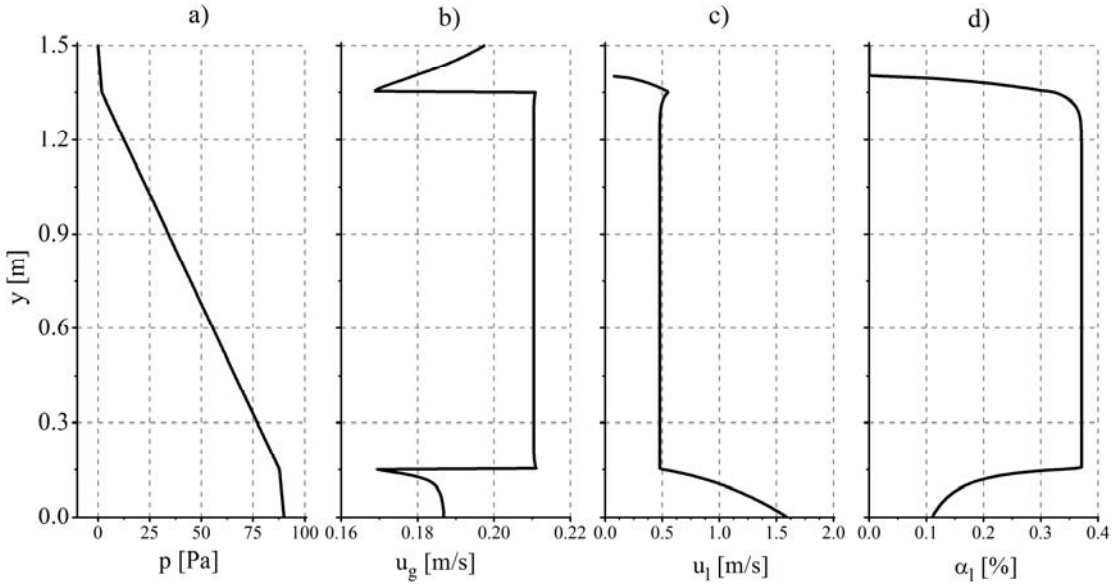

Fig. 3. Axial distributions of static pressure p (a), gas velocity u_g (b), liquid velocity u_l (c) and liquid volume fraction α_l (d)

Significant changes of flow resistance at the absorber sections influence the velocity fields of both media. The gas and liquid phases inside the porous zone keep constant velocities (see Fig. 3b,c). Additionally, due to the reduced actual column cross section area, gas velocity abruptly increases (see

Fig. 3b) on average by the factor of 1/ε, to satisfy the mass conservation. It should be noted that due to properties of the porous zone both fluids are uniformly distributed across the entire cross-section of the column resulting in practical absence of boundary layers. Outside the porous region the gas phase first falls down, and then slightly accelerates due to the reduced flow resistance (see Fig. 3b, the top and bottom sections). The flow in absorber column is dominated by the gas phase, which means that the liquid phase creates a film on the filling structure without blocking the gas flow. The distribution of the liquid volume fraction α_l shown in Fig. 3d confirms a minor role of the liquid phase, because α_l inside the porous region does not exceed 0.4%. Just below the porous zone the liquid content dramatically drops as a result of its acceleration, due to reduced flow resistance (see Fig. 3c,d).

Summing up, the results presented in this section show a physically justified behaviour of the countercurrent gas-liquid streams in the porous zone, thus proving the model's relevance and applicability to complex industrial processes.

3.2. Carbon dioxide absorption

As far as the absorber column performance is concerned the distributions of chemical species taking part in the reactions are of the utmost importance. Fig. 4 presents contour maps of reactants (Fig. 4a,b) as well as profiles of both reactants and products along the domain axis (Fig. 4c).

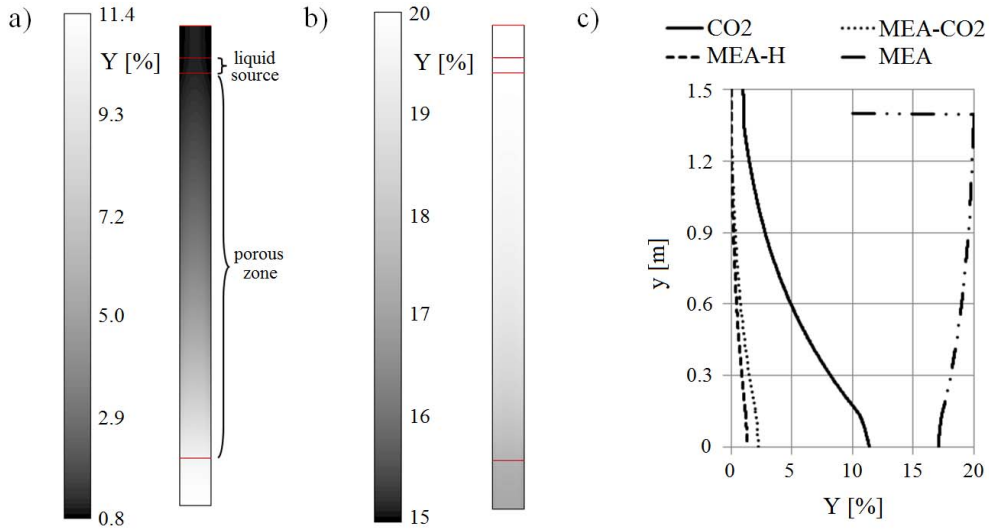

Fig. 4. Contour maps of CO_2 (a) and MEA (b) mass fractions as well as distributions of mass fractions of reactants and products along the domain axis (c)

One may easily notice a gradual decrease of CO_2 mass fraction (Fig. 4a) when passing vertically through the porous zone, as well as the accompanying change of MEA content (Fig. 4b). The inlet CO_2 content was 11.4% of flue gases, while at the outlet it fell down to 1% (see Fig. 4c), which means that for the applied parameters, capture efficiency reaches 91.5%. It should be noted, however, that the level of unloaded MEA at the outlet of the absorber is about 17% while at the inlet it was 20% (see Fig. 4c), hence only a small portion (about 15%) of MEA reacted with CO_2 for the above mentioned capture efficiency. Such a high ratio (approximately 6:1) between total and stoichiometric (needed to capture overall CO_2 stream) MEA fluxes results from the optimisation analysis taking into account the absorption efficiency, heat demand for the desorption and a power demand for the solvent circulation in the CCS system. For pilot installations (see for instance Godini and Mowla, 2008; Knudsen et al., 2009; Lee et al., 2008; Notz et al., 2007) operated at different conditions (flue gases composition, temperatures and fluxes) the excessive MEA flux lies in the range 80-90%. Fig. 4c additionally includes the distributions of reaction products, i.e. MEA carbamate (denoted as MEA-CO2) and protonated MEA (denoted as MEA-H). The molar concentrations of both reaction products must be the

same, as it results from the stoichiometry of absorption reaction (see Eq. 8b). However, the mass fraction profiles differ quantitatively as the molar mass of carbamate is greater than that of protonated MEA.

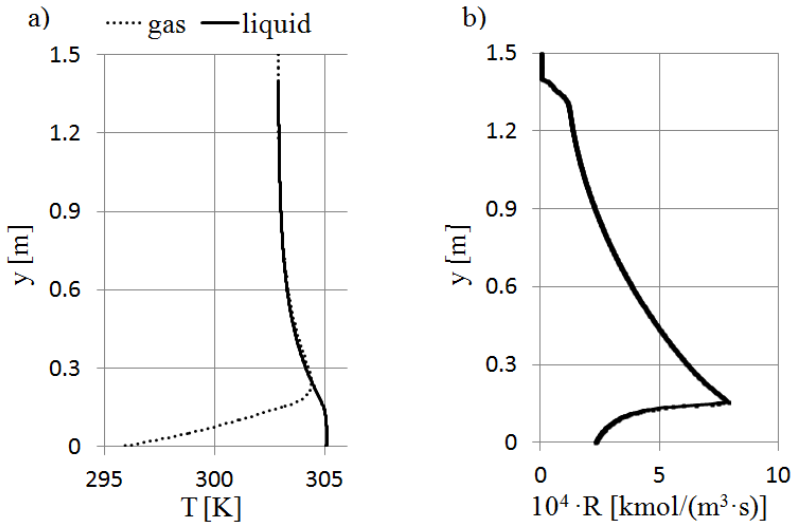

Fig. 5. Distributions of gas and liquid temperatures (a), and reaction rate (b) along the domain axis

As the reaction of CO_2 absorption by MEA is an exothermic process, it is of great importance to control the temperature field in the column. Its distributions are shown in Fig. 5a for both phases together, and additionally the reaction rate profile is presented in Fig.5b. As can be seen from Fig. 5a gas inlet temperature is noticeably lower than liquid temperature. Downstream the absorber inlet gas is warmed up reaching the temperature of liquid just after entering the porous zone. Starting from this point both phases keep the same temperature in the rest of the domain. A temperature profile of the liquid phase shown in Fig. 5a has a shape typical for absorber columns as demonstrated by experimental investigations as well as 1D simulation models (see e.g. Gaspar and Cormos, 2010; Harun et al., 2011).

Temperature distributions shown in Fig. 5a, as well as mass fraction profiles of reactants (see Fig. 4) correlate with the axial profile of reaction rate presented in Fig. 5b. As implied by Eq. (9) the intensity of absorption is proportional to the molar concentrations (i.e. to mass fractions) of reacting species, but also it is dependent on temperature according to Eq. (10). Moving down from the top of the column, the following tendencies may be noticed:

- mass content of MEA slightly decreases (Fig. 4b,c),
- mass content of CO_2 increases by one order of magnitude (Fig. 4a,c),
- temperature slightly grows (Fig. 5a).

All the above mentioned processes taken together lead to a significant growth of reaction rate, reaching its maximum at the bottom part of the porous zone.

3.3. Performance of absorption column for varying MEA regeneration level

At the next step the CO_2 capture model was used to perform a parametric study to show the performance of absorption column in varying conditions. Two parameters were selected for the analysis, i.e. the ratio of liquid and gas mass fluxes and the level of solvent regeneration in the stripper column. As it is known from the available literature the liquid-gas ratio is one of the key parameters governing CO_2 capture efficiency as well as the running costs of the CCS process (Godini and Mowla, 2008; Knudsen et al., 2009; Lee et al., 2008; Notz et al., 2007). The latter of the considered parameters is quite difficult to analyse, because the mass fractions of MEA and its absorption products (carbamate and protonated MEA) result from the thermo-chemical equilibrium achieved in the system and they

vary along the cycle. That means that with the present CO_2 absorption model (stripper neglected) it was not possible to capture the interactions between both parts of CCS installation. Thus the definition of inlet boundary condition in terms of solvent composition required an adoption of necessary information from source literature. The literature studies including reports from pilot CCS installations as well as simulation results (Faiz and Al-Marzouqi, 2009; Ferrara et al., 2009; Gaspar and Cormos, 2010; Mores et al., 2011) revealed a large scatter of information. For instance, Gaspar and Cormos (2010) using the simulation model developed within MATLAB/Simulink environment applied a 36% share of absorption products in the incoming solvent flux, which was measured at the pilot plant. The content of absorption products (loaded MEA) in total amine flux at absorber inlet varied in the range 0-50% depending on the literature source, and process conditions (see e.g. Faiz and Al-Marzouqi, 2009; Ferrara et al., 2009; Gaspar and Cormos, 2010; Mores et al., 2011). In the absence of precise information concerning MEA regeneration in stripper it was decided to conduct a series of simulations for varying level of loaded MEA at the absorber inlet. It was assumed that for all cases the molar fraction of amine and its products together was kept constant. The remaining solvent components (i.e. water and chemical additives) as well as flue gas composition were unchanged as well. The following three amine mixtures were considered:

- pure MEA (denoted as 100% MEA in Figs. 6 and 7),
- 75% MEA, 12.5% MEA-H, 12.5% MEA-CO2 (denoted as 75% MEA),
- 50% MEA, 25% MEA-H, 25% MEA-CO2 (denoted as 50% MEA).

Taking the above into account the pure MEA content in the aqueous solution was 20%, 15% and 10%, respectively.

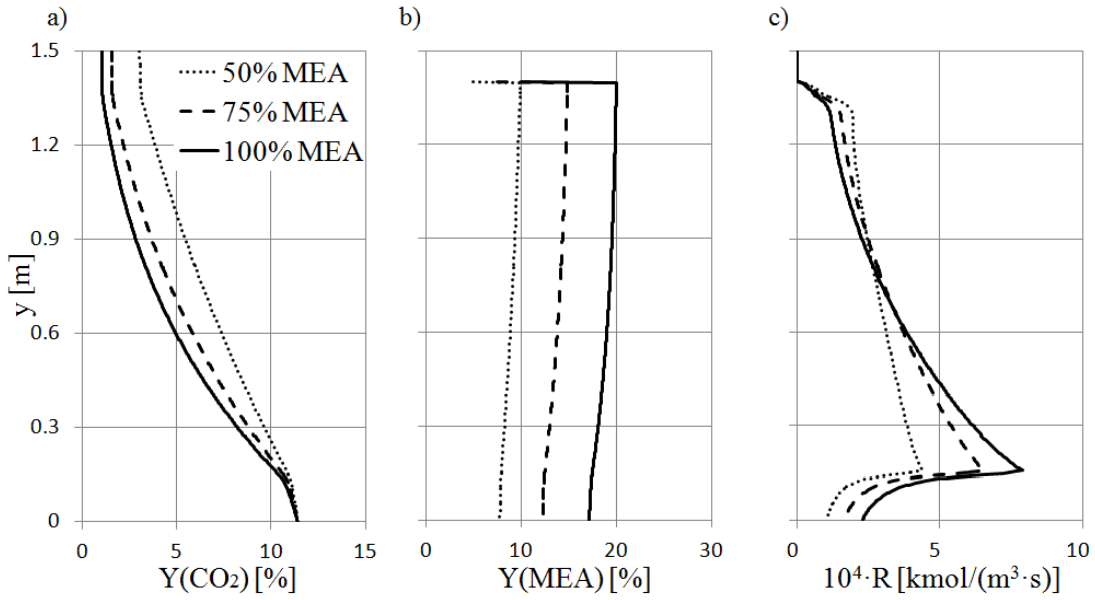

Fig. 6. Distributions of CO_2 (a) and MEA (b) mass fraction as well as reaction rate (c) for different inlet solvent composition along the column axis

With the use of the above stated solvent compositions simulations were conducted and their results are presented in Fig. 6 as the axial distributions of mass fractions of absorption reactants and of the reaction rate. As can be seen from Fig. 6a the growth of loaded MEA (absorption products, i.e. MEA-H and MEA-CO2, treated together) share leads to reduced CO_2 capture efficiency and for the analysed flue gas composition (11.4% CO_2 content) the outlet CO_2 level increases from approximately 1% to 3%. It is worth noticing, that the change of CO_2 content is nonlinearly related to the loaded solvent share. The change of the pure MEA content from 100% to 75% leads to the corresponding CO_2 increase from 1% to 1.5%, while its reduction from 75% to 50% (the same rate of change) doubles the CO_2 level (from 1.5% to 3%). The distributions along the column axis of the mass fraction of MEA are shown in Fig.

6b. Y(MEA) profiles corresponding to a varying content of loaded amine are nearly parallel and reveal a slight decrease in the downstream direction. The profiles of the reaction rate were collected in Fig. 6c to complement the already presented results. The increasing pure MEA content leads to the acceleration of absorption in the bottom part of the porous zone while it inhibits the reaction in the upper part of the column. It is interesting to note that all the reaction rate curves intersect at the same location inside the absorber (y≈0.8m). In order to explain the shapes of reaction rate distributions one should note that the absorption is a 2nd order reaction, which means that the molar fractions of reagents (MEA and CO_2) contribute linearly to the reaction rate. For all the inlet solvent compositions analysed the reaction rate reaches its maximum at the bottom of the porous zone and then decreases gradually towards the top of the absorber filling, while outside the porous region the reaction rate is abruptly decelerated (see Fig. 6c). The reaction rate is dominated by pure MEA content in the bottom part of the porous zone (where MEA fraction changes to a greater extent than CO_2 one), whereas by CO_2 concentration in the upper part (note that Y(CO_2) changes in a wider range than Y(MEA)). The demarcation line between the upper and bottom parts of the column (determined by the intersection of the reaction rate profiles) corresponds to the location where both influencing factors (i.e. CO_2 and MEA fractions) are in balance.

3.4. Model Validation

In order to validate CFD model of CO_2 capture it was decided to compare the simulation results with the available experimental data collected in the laboratory installation at IChPW Zabrze (see Krótki et al., 2012). As the most important parameter characterising the performance of CCS plant, CO_2 capture efficiency was defined as follows:

$$\eta = \frac{Q_{in} - Q_{out}}{Q_{in}} 100\% \tag{11}$$

where Q_{in} and Q_{out} stand for CO_2 mass fluxes at the absorber inlet and outlet, respectively.

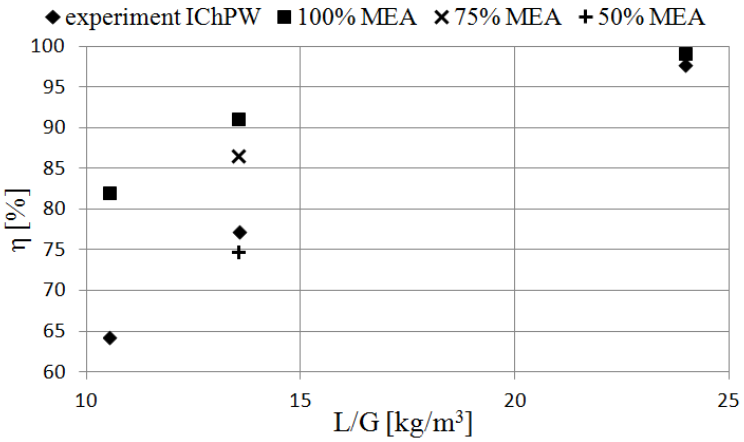

Fig. 7. CO_2 capture efficiency versus liquid to gas ratio - comparison of simulation and experimental data

CO_2 capture efficiencies for all the cases considered are collected in Fig. 7, together with the corresponding data from the laboratory installation (Krótki et al., 2012) as a function of liquid to gas ratio (L/G), representing the mass and volumetric fluxes of both phases. At first, the experimental data were compared to the simulation results obtained for 100% pure MEA content (corresponding to perfect MEA regeneration in the stripper). The capture efficiency increases along with L/G ratio both in the simulation and experiment. However, the CFD model overpredicted the data in comparison to results from laboratory installation. The discrepancies between these two sets of data were significant for low and intermediate L/G ratios, e.g. for L/G = 10.5kg/m^3 experimentally determined efficiency was equal to η = 64.2% while simulation provided the value of η = 82.1%. For the highest L/G ratio

considered the differences practically disappeared leading to very high capture efficiency, exceeding 97%. It should be noted that such high capture efficiencies (more than 90%) are not justified from the economical point of view, as they lead to excessive heat demand (Krótki et al., 2012) during the desorption stage. As discussed at the beginning of the present section, in real CCS installations an absorber is supplied with solvent containing certain portion of loaded MEA. So, it is believed that the absence of absorption products (i.e. carbamate and protonated MEA) in the solvent stream entering the absorber is the reason for the deviation of simulation results from experimental data. The results of the simulations conducted for the amine solution containing loaded MEA were additionally included in Fig. 7 for the L/G = 13.55kg/m^3. One may easily notice, that the increase of the loaded MEA content leads to reduction of CO_2 capture efficiency as discussed previously. For the case of 50% content of absorption products the efficiency determined from the simulation falls even below the efficiency level corresponding to the experimental conditions. It should be remarked here, that the actual value of loaded MEA content during the IChPW laboratory tests was not available, so this problem requires further research.

The simulation results presented in this paper and compared to the available literature and laboratory plant data seem to prove that the numerical model recovers the CO_2 capture in a reliable way and may be regarded as a useful tool in the analysis of absorber columns.

4. CONCLUSIONS

A CFD Euler-Euler multiphase model has been developed in order to simulate CO_2 capture from flue gases by chemical absorption by aqueous MEA solution in the porous zone. A complex flow system including countercurrent gas-liquid streams, chemical reaction and heat transfer has been successfully adopted and tested in typical operational conditions of a laboratory-scale absorber column. Simulations showed a realistic behaviour of the model both in terms of flow hydrodynamics as well as chemical absorption of CO_2. The model has been validated using reference experimental data showing good qualitative and quantitative agreement and proving its relevance. A series of simulations was performed, based on which the following observations were formulated:

- the model allowed to follow the process in detail, especially to investigate the distribution of key parameters along the column and their mutual relations,
- the reaction rate is mostly dependent on reacting species content and reaches its maximum value at the bottom of the column where CO_2 concentration is the highest,
- carbon dioxide capture efficiency is mostly influenced by the liquid to gas ratio (L/G) - a key process parameter; for increasing amine solvent flux capture efficiency grows reaching nearly 100% for $L/G \approx 25$ kg/m^3; however, the optimal L/G value, being the compromise between capture efficiency and the costs of the process, should be recommended within the range 12-16 kg/m^3,
- the concentration of loaded MEA at the inlet to the absorber column strongly affects the efficiency of CO_2 capture, that is why the desorption process should be precisely controlled enabling for the optimal performance of entire CCS installation.

The CCS numerical model is still being developed and it is planned to extend its functionality to the desorption stage covering a complete carbon dioxide capture cycle. The application of such a model will allow for more reliable process simulation and enable to formulate optimisation guidelines.

The research presented in this paper was funded by the National Centre of Research and Development in the framework of Contract SP/E/1/67484/10 - Strategic Research Programme - Advanced technologies for energy generation: Development of a technology for highly efficient zero-emission coal-fired power units integrated with CO_2 capture.

SYMBOLS

C	molar concentration, kmol/m^3
D_m	mass diffusion coefficient, s^{-1}
D_T	thermal diffusion coefficient, kg/(m^2·s)
F	phase interaction force, N/m^3
G	volumetric flux of gas phase, m^3/s
J	stream of species diffused, kg/(m^3·s)
L	mass flux of liquid phase, kg/s
M	molecular weight, kg/kmol
Q	heat flux exchanged between phases, W/m^3
Q	mass flux, kg/s
R	heterogeneous reaction rate, kg/(m^3·s)
Re	Reynolds number, -
S	mass source term, kg/(m^3·s)
S_e	enthalpy source term, W/m^3
S_{pz}	momentum sink term in porous zone, N/m^3
T	temperature, K
Y	mass fraction, kg/kg
h	specific enthalpy, J/kg
k_f	forward reaction rate constant, m^3/(kmol·s)
p	static pressure, Pa
t	time, s
u	velocity, m/s
y	axial coordinate, m

Greek symbols

α	volume fraction, m^3/m^3
ε	porosity (void fraction), m^3/m^3
λ	thermal conductivity, W/(m·K)
μ	dynamic viscosity, Pa·s
ρ	density, kg/m^3

Subscripts

CO2	denotes carbon dioxide
g (l)	denotes gas (liquid) phase
in	denotes inlet to the absorber
MEA	denotes monoethanolamine
out	denotes outlet from the absorber

REFERENCES

Alie C.F., 2004. *CO_2 capture with MEA: Integrating the absorption process and steam cycle of an existing coal-fired power plant*. MSc thesis, University of Waterloo, Waterloo, Ontario, Canada.

Asendrych D., Niegodajew P., Drobniak S., 2012. Modelling CO2 capture in post-combustion technology. *Nowa Energia*, 2, 156-157.

Astarita G., Savage D. W., Bisio A., 1983. *Gas treating with chemical solvents*. Wiley, New York.

Barth D., Tondre C., Delpuech J., 1986. Stopped-flow investigation of the reaction kinetics of carbon dioxide with some primary and econdary alkanolamines in aqueous solutions. *Int. J. Chem. Kinetics*, 18, 445-457. DOI: 10.1002/kin.550180404.

Basu S., 2001. Wall effect in laminar flow of non-Newtonian fluid through a packed bed. *Chem. Eng. J.,* 81, 323-329. DOI: 10.1016/S1385-8947(00)00221-7.

Billet R., 1995. Packed towers in processing and environmental technology. *VCH Verlagsgesellschaft mbH*, Weinheim.

Crespy A., Bolève A., Revil A., 2007. Influence of the Dukhin and Reynolds numbers on the apparent zeta potential of granular porous media, *J. Colloid Interface Sci.*, 305, 188-194. DOI: 10.1016/j.jcis.2006.09.038.

Faiz R., Al-Marzouqi M., 2009. Mathematical modelling for the simultaneous absorption of CO_2 and H_2S using MEA in hollow fiber membrane contractors, *J. Membrane Sci.*, 324, 269-278. DOI: 10.1016/j.memsci.2009.06.050.

Ferrara F., Cali G., Frau C., Pettinau A., 2009. Experimental and numerical assessment of the CO_2 absorption process in the Sotacarbo pilot platform, *1st International Conference on Sustainable Fossil Fuels for Future Energy – S4FE*.

Gaspar J., Cormos A-M., 2010. Dynamic modelling and validation of absorber and desorber columns for post-combustion CO_2 capture, *Comput. Chem. Eng. J*., 35, 2044-2052. DOI: 10.1016/j.compchemeng.2010.10.001.

Godini H. R., Mowla D., 2008. Selectivity study of H_2S and CO_2 absorption from gaseous mixtures by MEA in packed beds. *Chem. Eng. Res. Des.*, 86, 401-409. DOI: 10.1016/j.cherd.2007.11.012.

Harun N., Douglas P.L., Ricardez-Sandoval L., Croiset E., 2011. Dynamic simulation of MEA absorption processes for CO_2 capture from fossil fuel power plant. *Energy Procedia*, 4, 1478-1485. DOI: 10.1016/j.egypro.2011.02.014.

Knudsen J. N., Jensen J. N., Vilhelmsen P-J., Biede O., 2009. Experience with CO_2 capture from coal flue gas in pilot-scale: Testing of different amine solvents. *Energy Procedia*, 1, 783-790. DOI: 10.1016/j.egypro.2009.01.104.

Kothandaraman A, Nord L., Bolland O., Herzog H.J., McRae G.J., 2009. Comparison of solvents for post-combustion capture of CO_2 by chemical absorption. *Energy Procedia*, 1, 1373-1380. DOI: 10.1016/j.egypro.2009.01.180.

Krótki A., Więcław-Solny L., Tatarczuk A., Wilk A., Śpiewak D., 2012. Laboratory research studies of CO2 absorption with the use of 30% aqueous monoethanolamine solution. *Archiwum Spalania*, vol. 12, nr 4, 195-203.

Lawal A., Wang M., Stephenson P., Koumpouras G., Yeung H., 2010. Dynamic modelling and analysis of post-combustion CO_2 chemical absorption process for coal-fired power plants. *Fuel*, 89, 2791-2801. DOI: 10.1016/j.fuel.2010.05.030.

Lee S., Maken S., Park J-W., Song H-J., Park J.J., Shim J.-G., Kim J.-H., Eum H.-M., 2008. A study on the carbon dioxide recovery from 2 ton-CO2/day pilot plant at LNG based power plant. *Fuel*, 87, 1734-1739. DOI: 10.1016/j.fuel.2007.07.027.

Mores P., Scenna N., Musatti S., 2011. Post-combustion CO_2 capture process: Equilibrium stage mathematical model of the chemical absorption of CO_2 into monoethanolamine (MEA) aqueous solution. *Chem. Eng. Res. Des.*, 89, 1587-1599. DOI: 10.1016/j.cherd.2010.10.012.

Moser P., Schmidt S., Sieder G., Garcia H., Stoffregen T., 2011. Performance of MEA in long-term test at the post-combustion capture pilot plant in Niederaussem. *Int. J. Greenh. Gas Control* 5, 620-627. DOI: 10.1016/j.ijggc.2011.05.011.

Niegodajew P., Asendrych D., 2012. Numerical modelling of countercurrent gas-liquid flow through the packed bed. *Modelowanie Inżynierskie*, 14 (45), 108-115.

Notz R., Asprion N., Clausen I., Hasse H., 2007. Selection and pilot plant test of new absorbents for post-combustion carbon dioxide capture. *Chem. Eng. Res. Des.*, 85, 510-515. DOI: 10.1205/cherd06085.

Schiller L., Naumann Z., 1935. A drag coefficient correlation, *Z. Ver. Deutsch. Ing.*, 77-318.

Simon L.L., Elias Y., Puxty G., Artanto Y., Hungerbuhler K., 2011. Rate based modeling and validation of a carbon-dioxide pilot plant absorption column operating on monoethanolamine. *Chem. Eng. Res. Des.*, 89, 1684-1692. DOI: 10.1016/j.cherd.2010.10.024.

Vaidya P.D., Kenig E.Y., 2007. CO_2-alkanolamine reaction kinetics: A review of recent studies. *Chem. Eng. Technol.*, 30, 1467-1474. DOI: 10.1002/ceat.200700268.

Weiland R.H., Dingman J.C., Cronin D.B., Browning G.J., 1998. Density and viscosity of some partially carbonated aqueous alkanolamine solutions and their blends. *J. Chem. Eng. Data*, 43, 378-382. DOI: 10.1021/je9702044.

Xu Y., Paschke S., Repke J.-U., Yuan J., Wozny G., 2008. Portraying the countercurrent flow on packings by three-dimensional computational fluid dynamics simulations. *Chem. Eng. Technol.*, 31, 10, 1445-1452. DOI: 10.1002/ceat.200800273.

Zhao C.S., Duan L.B., Chen X.P. Liang C., 2010. Latest evolution of oxy-fuel combustion technology in circulating fluidized bed. *Proc. 20th Int. Conference on Fluidized Bed Combustion*, V.2009, Xian, China, 49-58.

Received 01 August 2012
Received in revised form 23 April 2013
Accepted 30 April 2013